The 14th World Conference on Earthquake Engineering
October 12-17, 2008, Beijing, China

LOCAL BUCKLING RESTRAINT CONDITION FOR CORE PLATES IN BUCKLING RESTRAINED BRACES

Ryota Matsui[1], Toru Takeuchi[2], Jerome F. Hajjar[3], Kohji Nishimoto[4], and Ian Aiken[5]

[1]*Doctoral Student, Dept. of Architecture and Building Engineering, Tokyo Institute of Technology, Tokyo, Japan*
[2]*Associate Professor, Dept. of Architecture and Building Engineering, Tokyo Institute of Technology, Tokyo, Japan*
[3]*Professor, Dept. of Civil and Environmental Engineering, University of Illinois at Urbana-Champaign, IL, USA*
[4]*Manager, Building Construction and Steel Structure Div., Nippon Steel Engineering Co. Ltd., Tokyo, Japan*
[5]*Principle, Seismic Isolation Engineering Inc., CA, USA*
Email: matsui.r.aa@m.titech.ac.jp, ttoru@arch.titech.ac.jp, jfhajjar@illinois.edu, nishimoto.kohji1@eng.nsc.co.jp, ida@siecorp.com

ABSTRACT:

Buckling Restrained Braces (BRBs) are commonly used as ductile bracing elements in seismic zones. A key limit state governing the BRB behavior is overall flexural buckling. However, when the wall thickness of the steel tube restrainer is relatively small compared to the cross section area of the core plate, the restraint conditions against the local buckling of the core plate can be critical for the stability and strength of the BRB. In this study, cyclic loading tests and numerical analyses on BRBs are carried out using various tube restrainer configurations, and local buckling restraint conditions are discussed using these results.

KEYWORDS: Buckling Restrained Brace, Local Buckling Failure, Restraint Performance

1. INTRODUCTION

Buckling restrained braces (BRB) comprise a steel core plate restrained by a concrete in-filled tube. Developed for practice in the 1980's in Japan, BRBs have been employed in more than three hundred buildings as ductile bracing members or hysteretic dampers. The conditions for the BRB to obtain a stable hysteresis can be classified as follows.

(a) When an axial force is applied to the core plate, the steel tube restrainer should have sufficient stiffness for preventing overall buckling.
(b) Since the core plate section expands when it is compressed in the plastic range, a certain amount of clearance must be provided between the core plate and the restrainer to prevent the core plate from prematurely bearing against the restrainer, thus transferring significant axial force to the restrainer through friction and potentially causing overall buckling of the BRB.
(c) The core plate slightly buckles within the above mentioned clearance, and out-of-plane force components are produced at each corner of the buckling wave. The walls of the restrainer should possess sufficient stiffness and strength to restrain the core plate.
(d) The connections at the both ends of the BRB must have sufficient stiffness and strength for the BRB to maintain stable performance under expected maximum force and deformation.
(e) The effective buckling length for designing BRB should be determined including considering the stiffness of the connections.

The condition of the BRB restrainer for preventing overall buckling (a) was discussed by Fujimoto, Wada et al. [1)], indicating that the core plate yield force need to be smaller than Euler's buckling force of the restrainer. The appropriate conditions for clearance between the core plate and the restrainer (b) were also discussed by Fujimoto, Wada et al.[1)] for a core plate within the rectangular steel tube, by Takeuchi, Suzuki et al. [2)] for a core tube with an outer tube restrainer. In their study, the condition of core plate local buckling (c) was discussed by using an elastic spring of in-filled mortar, and it was concluded that there are very few possibilities for local buckling failure in an ordinary BRB. The effect of the BRB connection stiffness (d) was researched by

Takeuchi, Yamada et al.[3]. K.C.Tsai et al.[4], and Roeder et al.[5]. The effective buckling length of BRBs was researched by Inoue et al.[7] by considering the stiffness of the connections (e).

However, for the conditions (c), it has been reported that there are risks of local buckling failure where the wall thickness of the restrainer and mortar thickness at the edge of core plate are relatively small compared to the sectional area of the core plate[8]. In such a case, the core plate buckles locally about the strong axis, the wall of the restrainer is not able to prevent it, as shown in Fig. 1, and such a failure can lead to overall buckling. In this study, BRBs with rectangular and circular tube restrainers with various thickness ratios are subjected to cyclic loading tests, and the behavior of the local buckling failure of the restrainer is investigated in these experiments and corroborating finite element method (FEM) analyses. This is followed by a proposal for the criteria preventing this failure mode.

2. BUCKLING CONDITIONS USING ELASTO-PLASTIC SPRING SUPPORT

When the effect of mortar between the edge of the core plate and the restrainer wall is negligible, the local buckling failure as shown in Fig. 1 can be modeled by the core plate being supported by double steel plates at the top and bottom in the direction of the strong axis as shown in Fig. 2.

The boundary condition at the corner of the restrainer wall is regarded as rigid, because the restrainer is filled with mortar. The spring coefficient β_r along axis is calculated by using eq. (1),

$$\beta_r = \frac{192 E_{tr} I_r}{B_r^3} \tag{1}$$

where E_{tr} is the tangent modulus of the restrainer wall, I_r, the moment of inertia per unit restrainer wall; B_r, the width of the restrainer wall, and the local buckling force of the core plate is evaluated by eq. (2).

$$P_{crl} = 2\sqrt{\beta_r E_{tc} I_c} \tag{2}$$

where E_{tc} is the tangent modulus of the core plate, I_c, is the moment of inertia of the core plate.

In the elastic range, the buckling force derived from eq. (2) is considerably larger than the yield strength of the core plate. However, after the yielding, the tangent modulus of the core plate E_{tc} and the spring stiffness β_r along the cyclic loading are reduced. Subsequently, the local buckling force P_{crl} also decreases and local buckling failure can occur when P_{crl} becomes smaller than the core plate yield force P_{cy}. For example, the material characteristic of the core plate and restrainer wall is depicted as in Fig. 3; the width of the restrainer is taken as

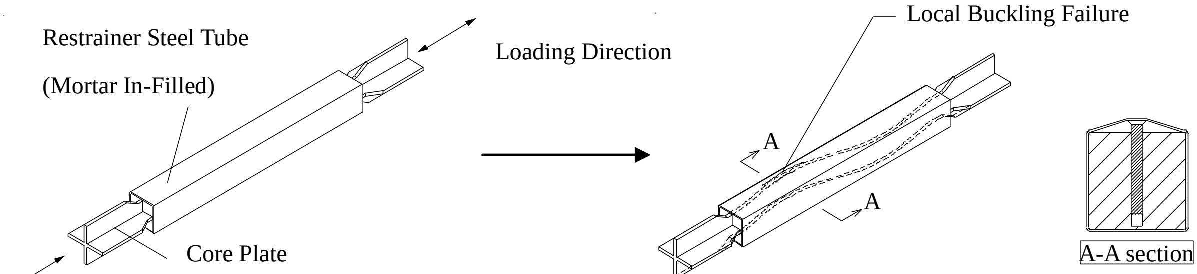

Fig 1 Local Buckling Failure in BRB

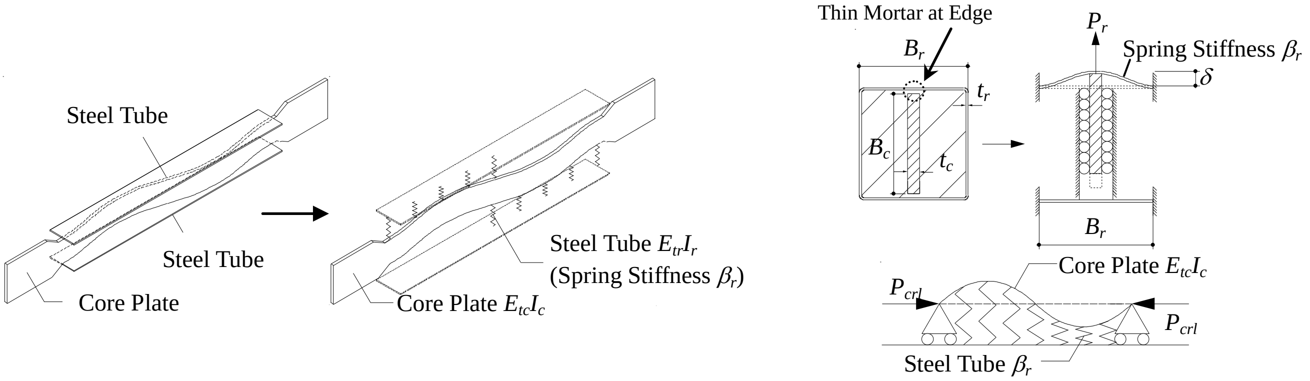

Fig. 2 Restrainer Wall Spring Model

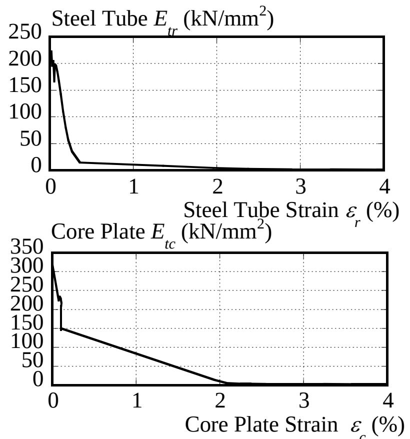

Fig. 3 Tangent Modulus Transition

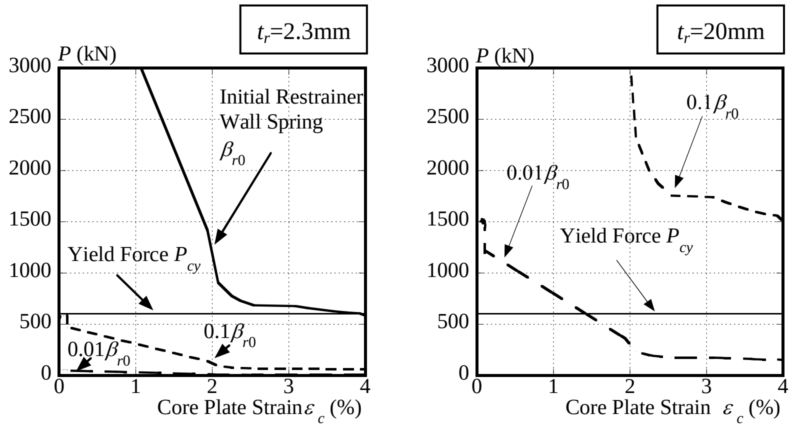

Fig. 4 Local Buckling Force of Core Plate

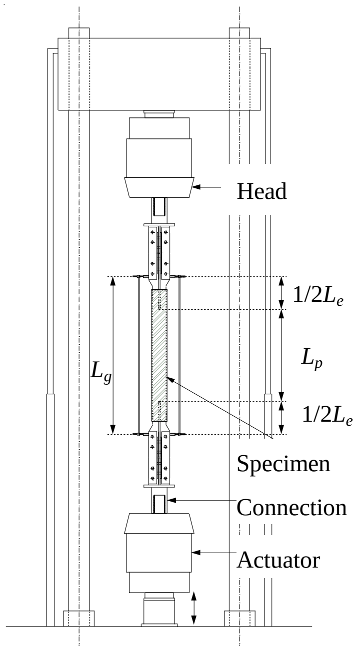

Fig. 5 Setup of Uniaxial Cyclic Loading Test

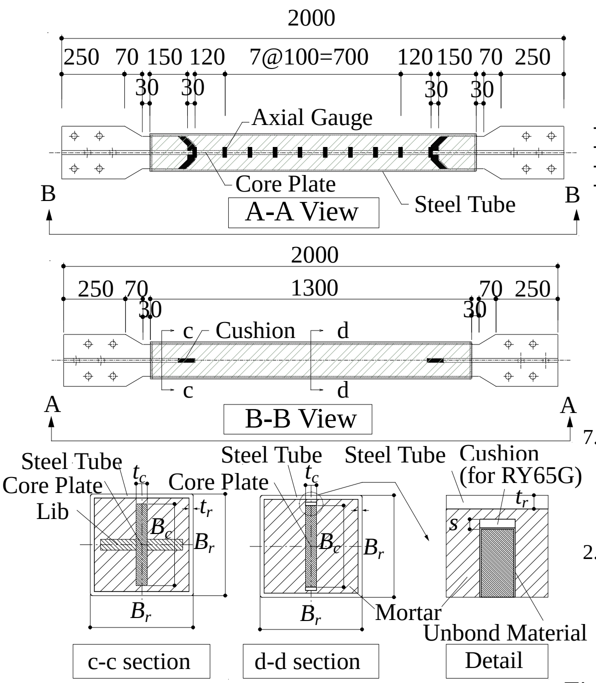

Fig. 6 Cyclic Loading Test Specimen

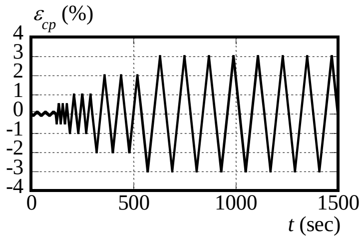

Fig. 7 Test Program of Uniaxial Cyclic Tests

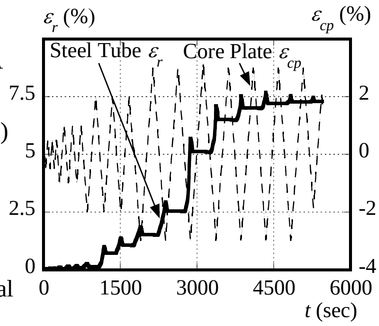

Fig. 8 Restrainer Strain Transition (RY65)

Table 1 Details of the Specimens in Uniaxial Cyclic Loading Tests

Specimen	B_r (mm)	t_r (mm)	Steel Tube	σ_{ry} (N/mm^2)	P_{crl} (kN)	B_c (mm)	t_c (mm)	Core Plate	σ_{cy} (N/mm^2)	P_{cy}(kN)	P_{crl}/P_{cy}	s (mm)	Local Buckling Failure
RY25	150	6	STKR400	350.2	1.92×10^5	130	16	SS400	261.0	542.9	613	1.0	None
RY65		2.3	SPHC-P	351.2	2.45×10^5						164	1.0	Occurred
RY65G												6.0	
CY83	165.2	2		231.2	2.01×10^5						110	1.0	None

150 mm and the thickness of the restrainer tube is taken as 2.3 mm and 20 mm, then the buckling force of the core plate can be obtained as shown in Fig. 4. In these conditions, local buckling failure is expected when the strain of the core plate exceeds approximately 2.0%, and the spring stiffness of the restrainer wall decreases to 1/10 or 1/100 of the elastic range.

3. UNIAXIAL CYCLIC LOADING TEST

3.1. Loading Conditions

To confirm the possibility of local buckling failure, cyclic loading tests on BRB were carried out at the University of Illinois at Urbana-Champaign. The setup of the uniaxial cyclic loading test is shown in Fig. 5. Both ends of the BRB are rigidly supported and a cyclic axial force is applied along its axis. The characteristic of the specimens are listed in Table 1 and Fig. 6. The core plate is 16x130, and a cushion piece is added only in

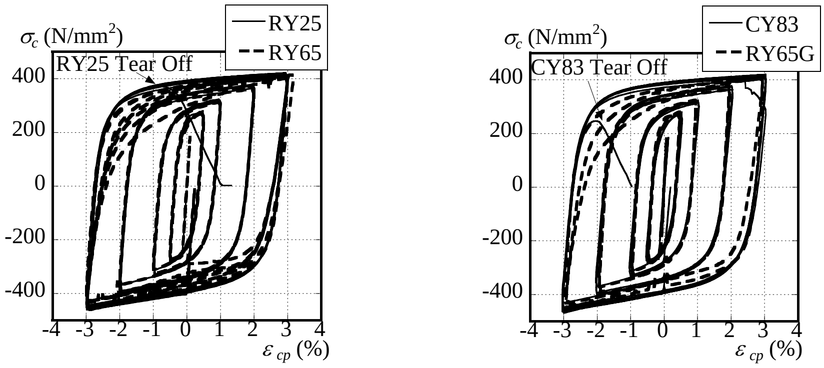

Fig. 9 Hysteretic Curve (Uniaxial Cyclic Loading Tests)

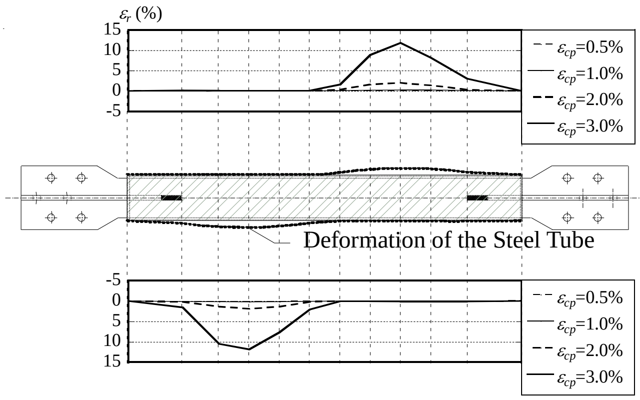

Fig. 10 Local Buckling Failure

Photo 1 Local Buckling Failure

RY65G at the edge of the core plate to increase the clearance and to clarify the effect of the clearance on local buckling failure. The loading program of the tests is shown in Fig. 7. The force applied to the BRB is measured by a load cell in the test machine, and axial displacement of the BRB is measured by extensometers installed between both end steel plates. The displacement of the plastic zone of the core plate is defined as δ_{cp} and is estimated by using eq. (3):

$$\delta_{cp} = \delta_g - \frac{P_c}{A_e E_{c0}} L_e \tag{3}$$

where δ_g is the initial extensometer displacement in L_g; the extensometer distance is shown in Fig. 5, P_c is the core plate axial force, A_e is the cross section of the core plate at connections, E_{c0} is the elastic modulus of the core plate, and L_e is the initial length of elastic zone in the connections. From these, the strain of the plastic zone of the core plate ε_{cp} is calculated by eq. (4), where L_p is the initial length of plastic zone:

$$\varepsilon_{cp} = \frac{\delta_{cp}}{L_p} \tag{4}$$

3.2. Result of Cyclic Loading

The surface strain of the buckling restrainer of RY65 along the loading is shown in Fig. 8, and the hysteretic curves obtained from the test are shown in Fig. 9. RY25 with a thick restrainer wall and CY83 with a circular restrainer showed no local buckling failure, and displayed stable stress strain curves until the fatigue fracture of the core plates. On the other hand, RY65 and RY65G with a thin restrainer showed local buckling failure at 2% strain amplitude (Photo 1). The local deformation of the restrainer wall grew significantly during the cyclic loading, and the test was stopped when the connection of the BRB became unstable due to the influence of the eccentric deformation. As shown in Fig. 8, the initial strain of the restrainer wall was not significant in early stage; however, it increased dramatically along the cyclic loading at amplitude of the strain greater than 2%. As in Fig. 9, the stiffness reduction occurred earlier in RY65G than in RY65. This means that the additional clearance besides the core plates influences local buckling failure. The distribution of strain along the restrainer wall is shown in Fig. 10; the figure indicates that the strain increases considerably where the out-of-plane

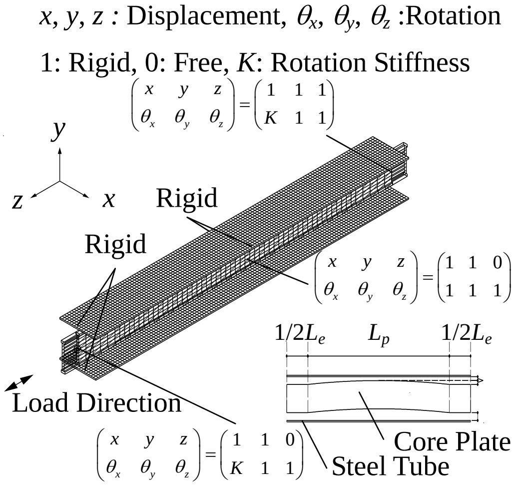

Fig. 11 FEM Analysis Model

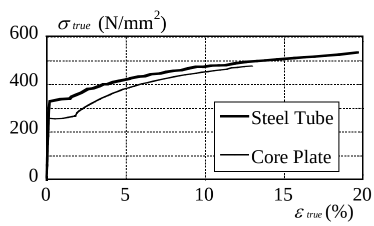

Fig. 12 Material Characteristic

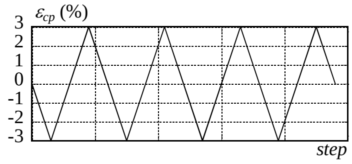

Fig. 14 Input Strain

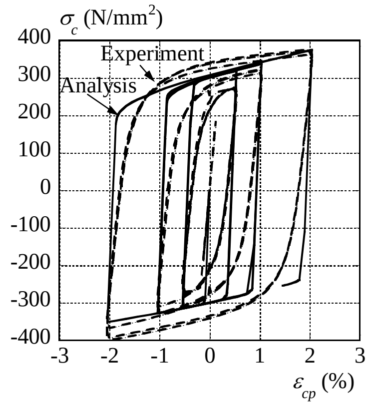

Fig. 13 Stress Strain Curve of RY65 (FEM versus Experiment)

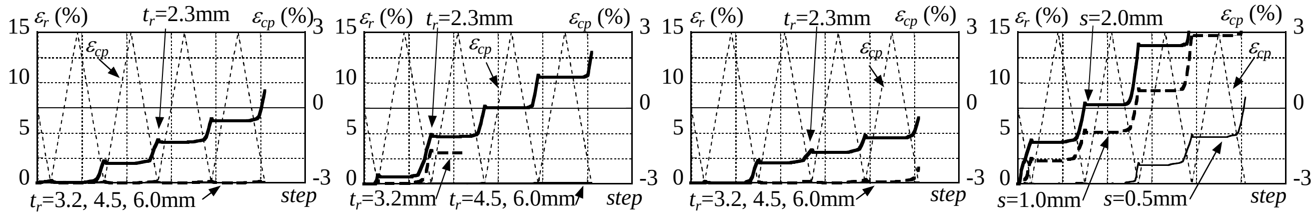

(a) s=0.5mm, L_p=1000mm (b) s=1.5mm, L_p=1000mm (c) s=2.0mm, L_p=1000mm (d) t_r=2.3mm, L_p=1000mm

Fig. 15 FEM Analysis Result

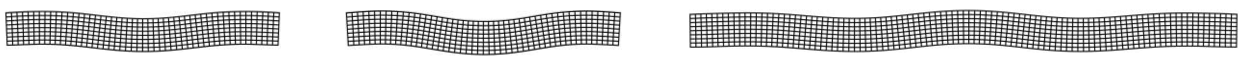

(a) s=0.5mm, L_p=1000mm (b) s=2.0mm, L_p=1000mm (c) s=0.5mm, L_p=2000mm

Fig. 16 Core Plate Deformation

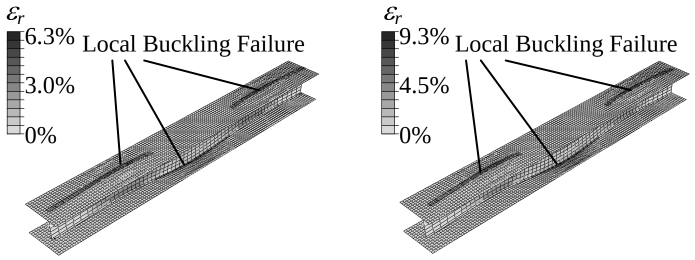

(a) s=0.5mm, L_p=1000mm (b) s=2.0mm, L_p=1000mm

Fig. 17 Restrainer Contour t_r=2.3mm

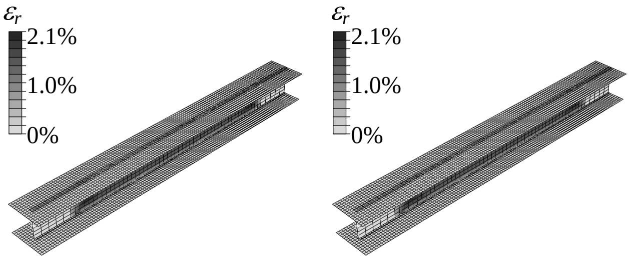

(a) t_r=3.2mm, L_p=1000mm (b) t_r=4.5mm, L_p=1000mm

Fig. 18 Restrainer Contour s=0.5mm

deformation of the restrainer is observed.

The restrainers were disassembled after the tests and the core plate of RY25 and CY83 showed no local buckling. On the other hand, the core plate of RY65 and RY65G showed significant wave deformation about strong axis with the mode in Fig. 10.

4. FEM ANALYSIS OF LOCAL BUCKLING FAILURE

To clarify the local deformation behavior of the restrainer, FEM analyses were carried out. ABAQUS Ver. 6.5-6 was used for analysis, and various models following previous tests are analyzed as follows. Because the mortar was observed to have very limited contribution to the restraint, the core plates are modeled as directly touching the restrainer walls in the analyses, as in Fig. 11. The deformation of the weak axis and the rotation of the core plate are restrained, and the initial irregularities are introduced to the core plate within the clearance between the core plate and the mortar. A shell element is used for modeling the core plate and restrainer walls, and each

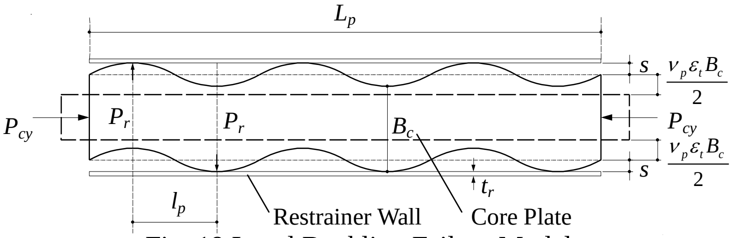

Fig. 19 Local Buckling Failure Model

Fig. 20 Plastic Zone of Restrainer Wall

element is divided into an approximately regular hexahedron. The material characteristics are modeled as shown in Fig. 12 following coupon test results. In Fig. 13, the hysteretic curves obtained from an analysis are compared with that of the cyclic loading experiment. Both results generally agree, and these analyses are simulating well the behavior of the local buckling failure of the restrainer. Various models changing the thickness of the restrainer wall, the clearance between the core plates and the length of the plastic zone of the core plate were prepared, and a constant cyclic load as shown in Fig. 14 was applied.

The strain transition in each case is shown in Fig. 15. The local deformation increases earlier when the restrainer was thinner, and the clearance between the core plate and the restrainer is larger. On the other hand, the length of the plastic zone of the core plate does not affect on the local deformation behavior. The half length of the local buckling wave of core plate was kept around $3.5B_c$~$5B_c$ even when the plastic zone length of the core plate changed, as shown in Fig. 16. The strains of the restrainer walls are compared in Fig. 17 and Fig. 18, where local buckling failure is observed when the thickness of the restrainer walls is smaller and the clearance between the core plate and the restrainer is larger.

5. DISCUSSION ON LOCAL BUCKLING FAILURE CRITERIA

From the results of the experiments and analyses, the length of the local buckling waves of the core plate varies approximately between $3.5B_c$ and $5B_c$. The reason for this behavior is explained as follows. When the core plate buckles within the restrainer as shown in Fig. 19, the number of buckling waves increases with the additional axial force, however they stop increasing at the point where Euler buckling forces resulting from the tangent modulus of the core plate reaches the yield strength of the core plate σ_{cy}, as described by Eq. (5):

$$\sigma_{cy} = \frac{P_{cy}}{A_c} = \sigma_{cr} = \frac{\pi^2 E_{tc}}{\bar{\lambda}^2} \tag{5}$$

where A_c is sectional area of core plate, E_{tc} is tangent modulus of core plate, and $\bar{\lambda} = l_p/i_c$ where i_c is radius of moment of inertia of the core plate. The length of local buckling wave is then determined as eq. (6):

$$l_p = i_c \bar{\lambda} = \frac{\pi B_c}{2}\sqrt{\frac{E_{tc}}{3\sigma_{cy}}} \tag{6}$$

The length of local buckling wave l_p is determined by the width of core plate and the tangent modulus in the plastic range. Where E/σ_{cy}=832 and the tangent modulus E_{tc}=0.02E, the length of the local buckling wave becomes approximately $l_p = 4B_c$. In the tensile stage, the section of the core plate decreases by $v_p \varepsilon_t B_c$, with the plastic Poisson's ratio v_p=0.5. The clearance between the core plate and the restrainer increases by the half of this value. The perpendicular force components working on the restrainer wall can then be calculated by employing eq. (7):

$$P_r = \frac{2s + v_p \varepsilon_t B_c}{l_p} P_{cy} = \frac{2s + v_p \varepsilon_t B_c}{l_p} B_c t_c \sigma_{cy} \tag{7}$$

From the FEM analyses, the length of the zones of the restrainer resisting against this force component is estimated to be approximately equal to the width of the restrainer as shown in Fig. 20. By estimating the collapse mechanism of the restrainer walls as shown in Fig. 21, the ultimate strength resisting the perpendicular force component can be calculated by using eqs. (8) and (9).

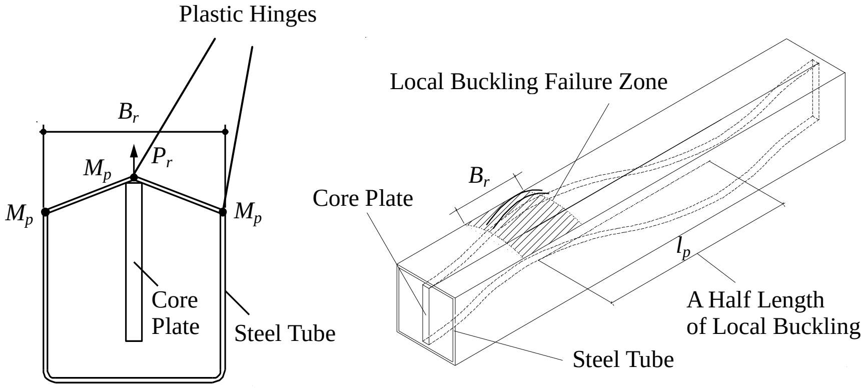

Fig. 21 Local Buckling Failure Mechanism

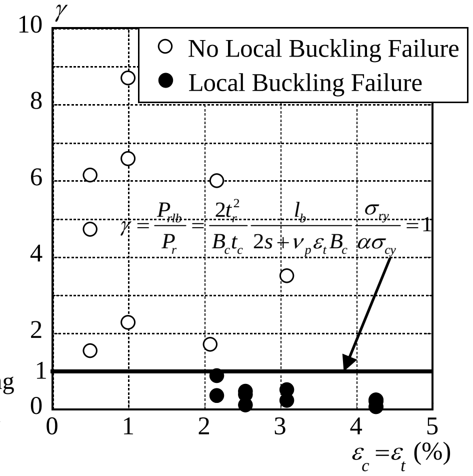

Fig. 22 Condition Confirmation

$$M_p = \frac{B_r t_r^2}{4}\sigma_{ry} \tag{8}$$

$$P_{rlb} = \frac{8M_p}{B_r} = 2t_r^2\sigma_{ry} \tag{9}$$

Here σ_{ry} is the yield stress of the restrainer wall. The ratio γ is then defined by eq. (10) as the ultimate strength of the restrainer wall P_{rlb} divided by the perpendicular force component of the core plate P_r:

$$\gamma = \frac{P_{rlb}}{\alpha P_r} = \frac{2t_r^2}{B_c t_c}\,\frac{l_p}{2s+v_p\varepsilon_t B_c}\,\frac{\sigma_{ry}}{\alpha\sigma_{cy}} \tag{10}$$

Here ε_t is the maximum tensile strain of the core plate, and α is strength increasing ratio after yielding (α=1.2~1.4). The ratio γ represents the safety factor against local buckling failure, and the axial force P_{lb} causing the local buckling failure can be calculated from eqs. (11) and (12) as follows:

$$P_{lb} = 2t_r^2\,\frac{l_p}{2s+v_m\varepsilon_t B_c}\,\sigma_{ry} \tag{11}$$

$$\gamma = \frac{P_{lb}}{\alpha P_{cy}} \tag{12}$$

The γ indexes estimated from the specimens of previous tests are shown in Fig. 22 together with occurrence of local buckling failure. From this figure, it is observed that all specimens with γ < 1.0 caused local buckling failure, and the criteria for the restrainer wall can be explained well by this index.

6. CONCLUSIONS

In this study, experiments and numerical analyses were carried out using BRB members with various restrainers, and the phenomenon of local buckling failure in these specimens was investigated. As a result, the following conclusions were obtained:

1) When the restrainer steel tube of the BRB is assumed to be an elastic spring, no local buckling failure of restrainer tube is expected. However, when the tangent modulus of the core plate and the restrainer wall are decreased in the plastic range, the possibility of local buckling failure increases.
2) Cyclic loading tests were carried out on BRB specimens with various restrainer thicknesses with thin mortar at the edge of the core plate, and local buckling failures were observed in specimens possessing rectangular tubes with a diameter-to-thickness ratio of 65. A significant increase in the strain on the restrainer wall was observed during cyclic loading. On the other hand, specimens containing a rectangular

tube with a diameter-to-thickness ratio of 25 and a circular tube with a diameter-to-thickness ratio of 83 did not cause local buckling failure.

3) From the FEM analyses, the increase of restrainer wall is confirmed to become more significant with a thinner restrainer wall and a larger clearance between the edge of the core plate and the restrainer. On the other hand, the length of the core plate does not affect on the local buckling behavior, and local buckling wave lengths are restricted to approximately 4.0 times of the core plate width.
4) The local buckling wave length of the core plate can be well explained by the generalized slenderness ratio calculated by using the tangent modulus. Considering the restrainer wall and the maximum tensile strain of the core plate, the criterion for local buckling restraint failure is provided. The proposed condition agrees well with the results of the experiments, and it is considered to be valid for the practical design of BRBs.

ACKNOWLEDGEMENT

This material is based upon work supported by Nippon Steel Engineering Co., Ltd. and the University of Illinois at Urbana-Champaign. The authors express thanks to Matthew Eatherton, Grzegorz Banas, and Tim Prunkard for their contributions to this research and experiments. Any opinions, findings, and conclusions or recommendations expressed in this material are those of the authors and do not necessarily reflect the views of the sponsors.

REFERENCE

Morihisa Fujimoto, Akira Wada, Eiichiro Saeki, Toru Takeuchi, and Atsushi Watanabe, “Development of a Buckling Restrained Brace,” *Quarterly Publication Column*, No.115, pp. 91-96, Sep., 1991 (in Japanese)

K. Suzuki, T. Takeuchi, T. Marukawa, Y. Kimura, T. Sugiyama, T. Ogawa, S. Kato, “Buckling Behavior of Compressive Tubular Columns with Additional Buckling Restrainer,” *International Symposium on Shell and Spatial Structures*, pp. 45-52, Sep., 2005

Toru Takeuchi, Satoshi Yamada, Madoka Kitagawa, Kazuaki Suzuki, and Akira Wada, “Stability of Buckling Restrained Braces Affected by the Out-of-plane Stiffness of the Joint Element,” *Journal of Structure and Construction Engineering*, AIJ, No. 575, pp. 121-128, Jan., 2004 (in Japanese)

Keh-Chuyan Tsai, Po-Chien Hsiao, Kung-Juin Wang, Yuan-Tao Weng, Min-Lang. Lin, Ker-Chun Lin, Chui-Hsin Chen, Juin-Wei Lai, Sheng-Lin Lin, “Pseudo-dynamic Tests of a Full Scale CFT/BRB Frame-Part I :Specimen design, experiment and analysis,” *Earthquake Engineering and Structural Dynamics*, 2008; 37:1081-1098 DOI: 10.1002/eqe.804

Charles W. Roeder, Dawn E. Lehman, and A. Christopoulos, “Seismic Performance of Earthquake-Resistant Steel Braced Frames with Buckling Restrained Braces.,” Proc., *8th U. S. National Conf. on Earthquake Engineering*, Earthquake Engineering Research Institute, Oakland, Calif., Paper No. 1503

Hideaki Tembata, Yuji Koetaka, and Kazuo Inoue, “Out-of-plane Buckling Load of Buckling Restrained Braces Including Brace Joints,” *Journal of Structure and Construction Engineering*, AIJ, No. 581, pp. 127-134, Jul., 2004 (in Japanese)

Mamoru Iwata, Ryo Murase, Youji Izumita and Masatoshi Murai, “Experimental Study on Buckling-Restrained Braces Using Steel Mortar Planks – Part3 Buckling Behavior of Core Plate-,” *Journal of Structure and Construction Engineering*, AIJ, No. 611, pp. 133-139, Jan., 2007 (in Japanese)